AD647085

Submitted by:

TRG, A Division of
Control Data Corporation
Route 110
Melville, New York 11746

AMPHIBIOUS VEHICLE STUDIES

Under Contract No. Nonr-4650(00)

Distribution of this document is unlimited.

Submitted to:

Office of Naval Research
Department of Navy
Code 438
Washington, D.C. 20360

DDC

FEB 23 1967

A

Reproduction in whole or in part is permitted for any
purpose of the United States Government.

June 1966

Submitted by:

TRG, A Division of
Control Data Corporation
Route 110
Melville, New York 11746

AMPHIBIOUS VEHICLE STUDIES

Under Contract No. Nonr-4650(00)

Distribution of this document is unlimited.

Submitted to:

Office of Naval Research
Department of Navy
Code 438
Washington, D.C. 20360

June 1966

TABLE OF CONTENTS

LIST OF FIGURES

ii

ACKNOWLEDGEMENT

The author is indebted to Mr. A.I. Raff, Mr. J.G. Koelbel and Mr. G. Sammis of TRG for their assistance in preparing this report, and to Mr. H. Dugoff of Davidson Laboratory for supplying resistance data on Davidson Laboratory's model.

1. INTRODUCTION

TRG's program calls for theoretical and experimental work on resistance and resistance reduction, and on improved flow to the grousers. We began by examining the data in [2], including the components of resistance and the dependence of resistance on test conditions. Also, in order to establish a connection with test data other than that on LVTP5 models we correlated that model test data with the extensive tests of Hay [1] on parallelopipeds. This work is described in Section 2. We then attempted to find a mathematical model (source or dipole distribution) of the LVTP5, such that the calculated resistance and body shape would agree sufficiently well with LVTP5 data to serve as a basis for studying shape modifications and their effect on resistance and flow. This work is described in Sections 3 and 4. We have begun to investigate bow shape modifications. We are aiming at the design of compatible devices for bow modification, which may be deployable, inflatable or useable for fuel or other fluid storage, and which perform their hydrodynamic tasks without degrading vehicle functions. This work is described in Section 6.

2. ANALYSIS OF LVTP5 MODEL TEST DATA

Figure 2.1 shows 1/4-scale model resistance in pounds versus model speed, full-scale speed and Froude number for:

a) LVTP5 model X-100, 1250 lbs. displacement (80,000 lbs. full scale) level trim, tracks run at zero slip, as reported in [2]. The curve is slightly faired from test points.

b) LVTP5 model built and tested by Davidson Laboratory, full scale displacement 82,500 lbs., embodying tread envelope but no treads or grousers. Model built to 1/12-scale, data expanded to 1/4-scale by Froude scaling neglecting frictional resistance. Data supplied by Davidson Laboratory.

c) LVTP5 model X-100, as in a) above, with tracks stationary.

We use Froude scaling neglecting frictional resistance because frictional resistance is estimated to be less than 10% in all relevant cases while resistance is not uniquely defined to within 10% because of varying test conditions. The difference between the three curves in Figure 2.1 is believed to be due mainly to the different treatment of the tracks. Scale effect and minor model shape differences are believed to be unimportant. The difference between the curves is substantial. Tests at other displacements, reported in [2], also show a substantial variation of towing resistance with track slip.

STEVENS: (82,500 LB FULL SCALE), TRIM EQUAL TO
FULL SCALE MEASURED TRIM, NO TREADS,
EXPANDED FROM 1/12 SCALE

X-100(A): 1250 LB (80,000 LB FULL SCALE), LEVEL TRIM,
TRACKS RUN AT ZERO SLIP, 1/4 SCALE

X-100(B): AS ABOVE, BUT TRACKS STATIONARY
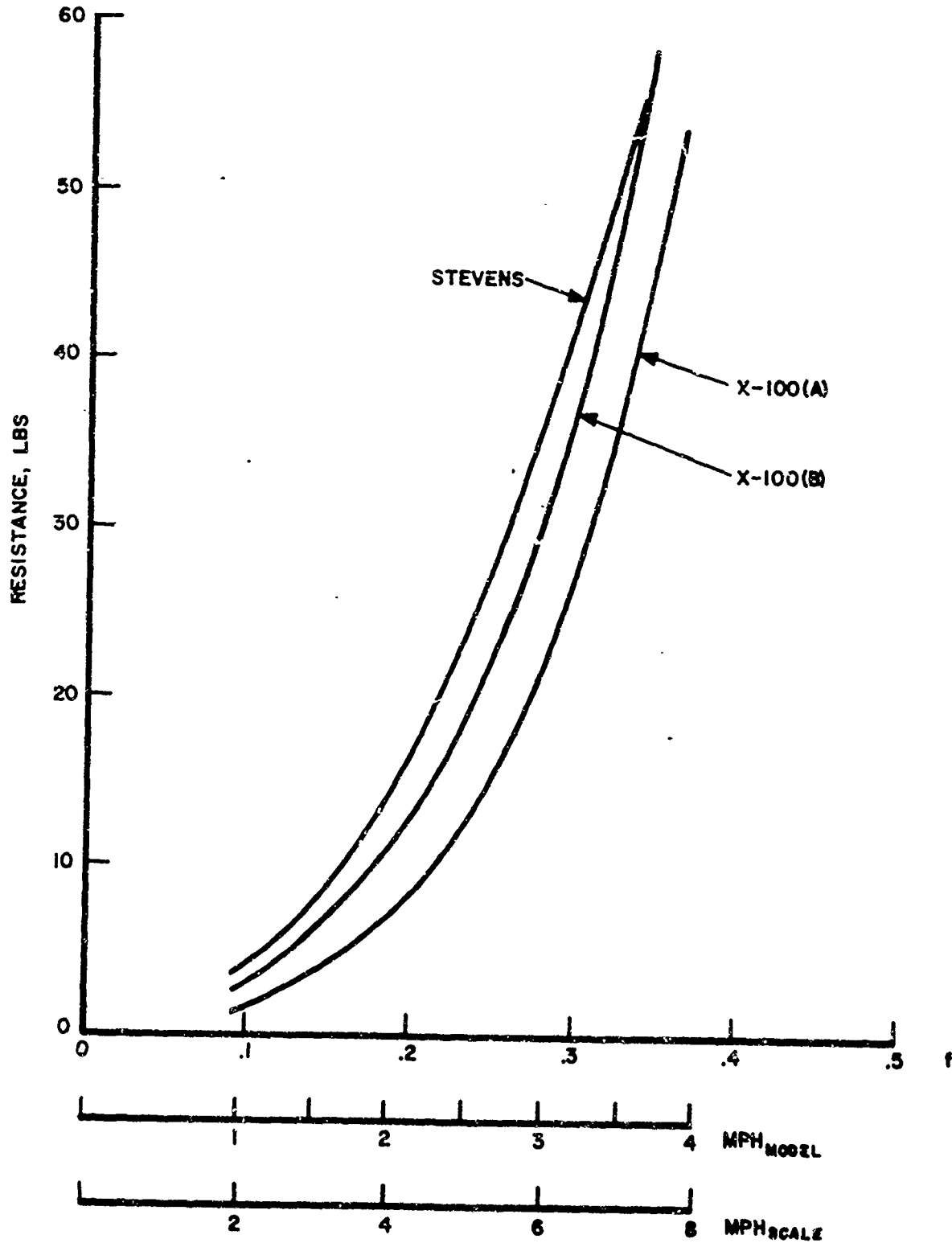
Figure 2.1

Total Resistance of Three LVTP5 Models

Figure 2.2 shows drag coefficient $C_D = R/\frac{1}{2}\rho v^2 A$, where A is static submerged frontal area, for

a) LVTP5 model X-100 as described in a) above,

b) LVTP5 model built by Davidson Laboratory, as described in b) above,

c) LVTP5 model X-100 as described in c) above,

d) a fully submerged flat plate whose aspect ratio is that of the LVTP5 (single or double model, C_D being insensitive to aspect ratio in this range),

e) a surface-piercing flat plate whose static submerged aspect ratio is that of model X-100 (B/H = 2.40),

f) an unrounded block, interpolated and Froude scaled from the report of Hay [1], B/H = 2.40, L/B = 3.

g) a block having rounded forefoot (forefoot radius/static draft = .6), interpolated and Froude-scaled from [1], B/H = 2.40, L/B = 5 ,

h) as f) above but with forefoot radius/static draft = 2.4 , L/B = 5 .

With reference to e), f), g) we note that the data depends weakly on L/B in this range of L/B. Also a), b), c) use the same value of A.

Examining Figure 2.2 we see

a) all the coefficients are speed-dependent,

b) rounding a block in various ways reduces the resistance by a factor of 2 or more.

We tentatively identify the quantity $C_R - C_R^{ZERO\ SPEED}$, the speed-dependent part of C_R, with wave resistance, keeping in mind that the coefficients of friction and separation drag are independent of Reynolds number in this range of Reynolds number
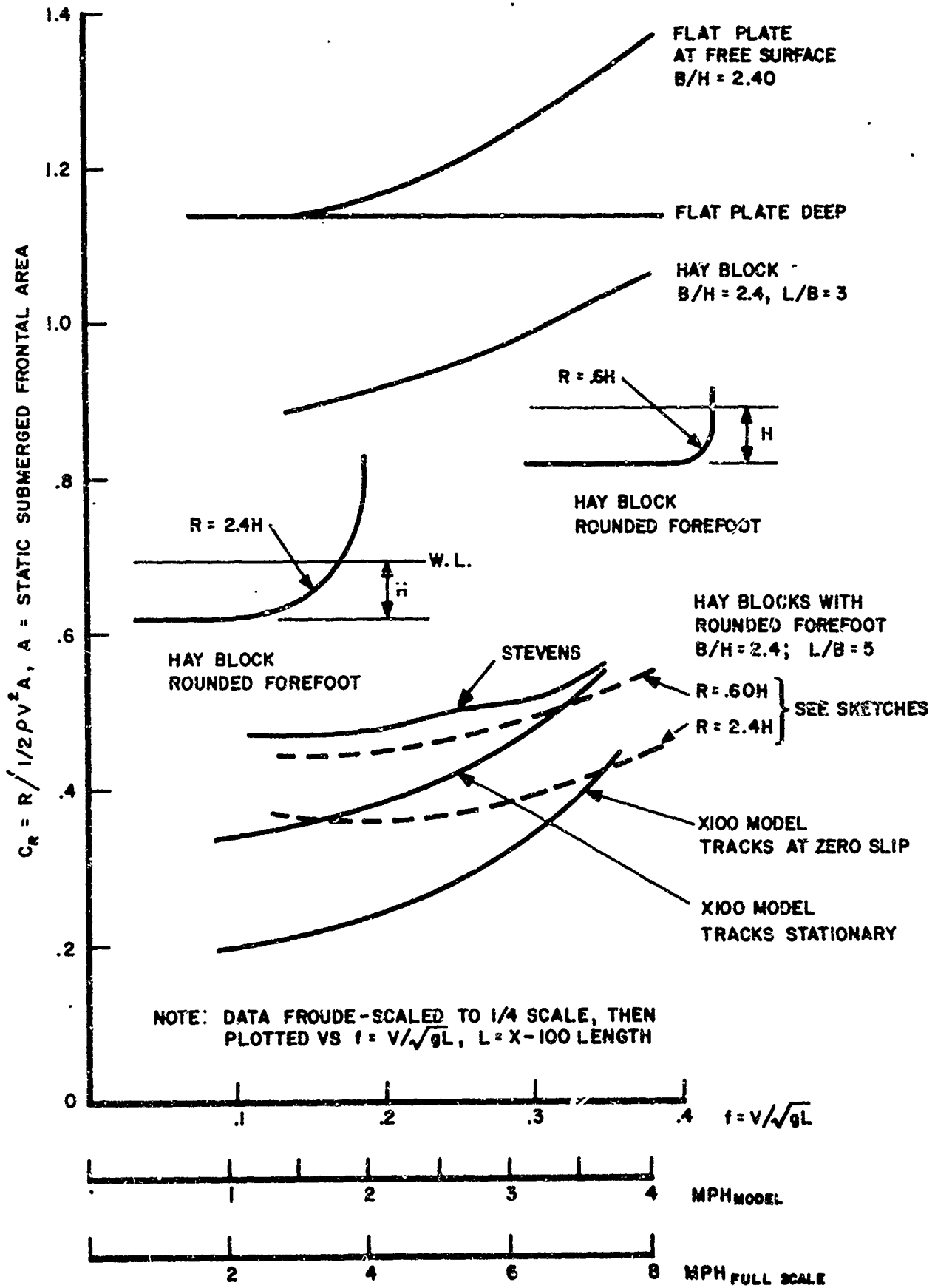
Figure 2.2

Total Resistance Coefficients of

Three LVTP5 Models and Various Blocks

We are encouraged to make this identification by the fact that
the low-speed asymptote of C_D for a flat plate is in fact equal
to C_D in the absence of a free surface. This quantity is plotted
in Figure 2.3, for three LVTP5 models. We see that the result
is almost identical for the X-100 models with the tracks run at
zero slip and held stationary, which is plausible. The Stevens
results are much lower. We are unable to account for the
difference in test results on the basis of differences in con-
figuration and test conditions. Since we are attempting to
predict the wave resistance theoretically the difference is vital.
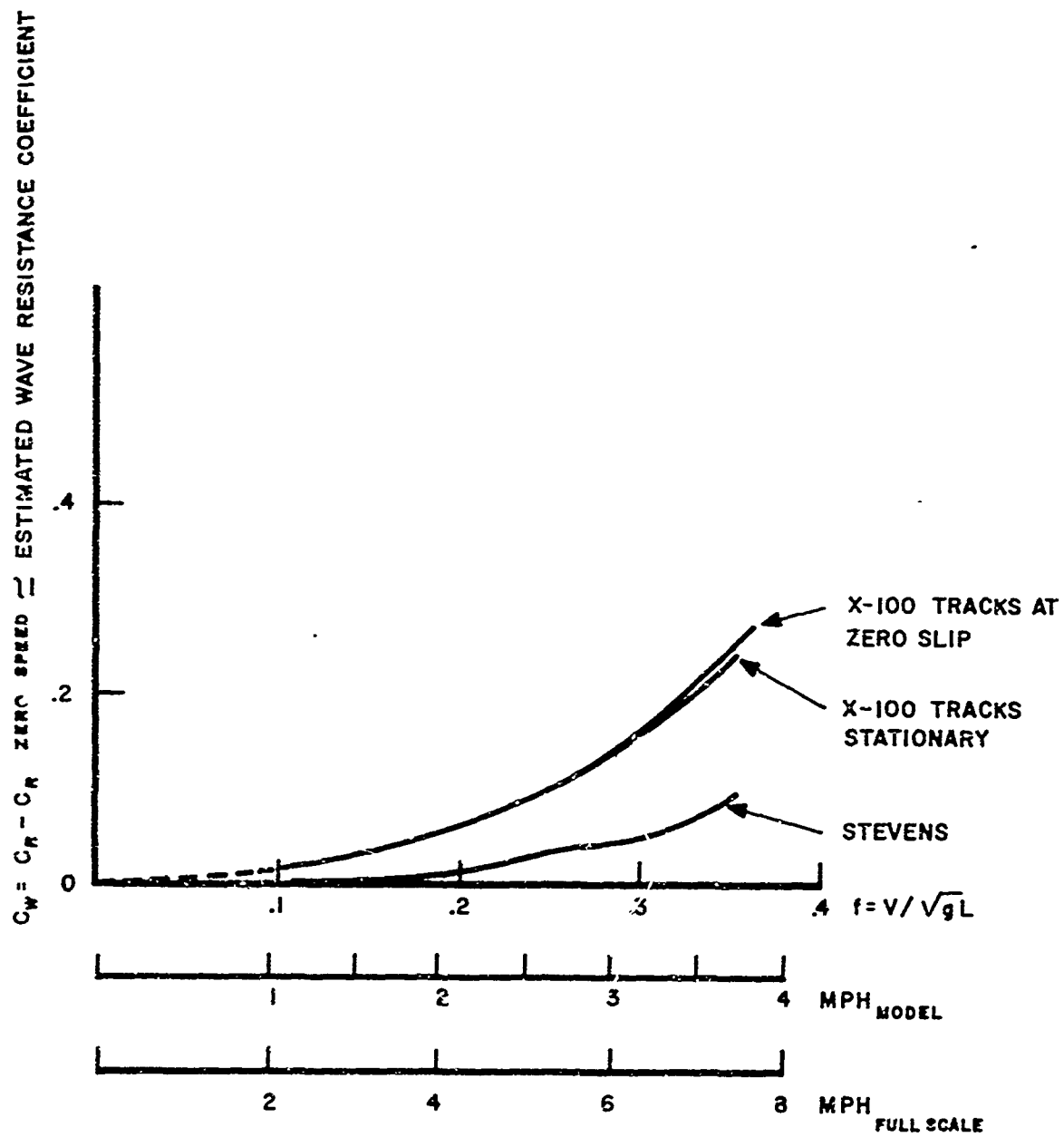
Figure 2.3

Wave Resistance Coefficients of Three LVTP 5 Models

3. RESISTANCE CALCULATIONS

The objective of these calculations is to help determine the validity of mathematical models (source or dipole distributions) of model X-100, as regards wave resistance. The validity of the models as regards the shape of model X-100 is discussed in Section 4. Estimated wave resistance coefficients from LVTP5 model tests were plotted in Figure 2.3

We are looking for dipole distributions whose calculated wave resistance approximates the measured model wave resistance. Since the theoretical model does not allow for tracks and since the waves made by this blunt vehicle may be nonlinear and therefore not calculated correctly we do not seek a very close approximation.

Before proceeding further we mention the result of an examination of the effect of varying beam on the wave resistance of blocks, keeping draft, length and speed fixed. In thin-ship theory the wave resistance varies as B^2, while for ships the measured data varies like B^n, where n varies but is generally between 1.5 and 2. The data in [1] indicates that for blocks having L/H = 5.72 the resistance is roughly proportional to $B^{1.0}$ at full scale speeds above 4 MPH, in the range $1.5 \leq B/H \leq 3.0$ or $.263 \leq B/L \leq .526$ (see Figure 3.1). This is a measure of the extent to which we are out of the thin-ship domain.

Wave resistance calculations were made for the LVTP5 model X-100, having the following characteristics:

Displacement ($\rho g \Psi$)	1250 lbs. (fresh water)
Length (L)	7.5'
Beam (B)	3.0'
Draft (H)	1.25' (to hull bottom)
δ = H/L	.167
B/2L = .2	
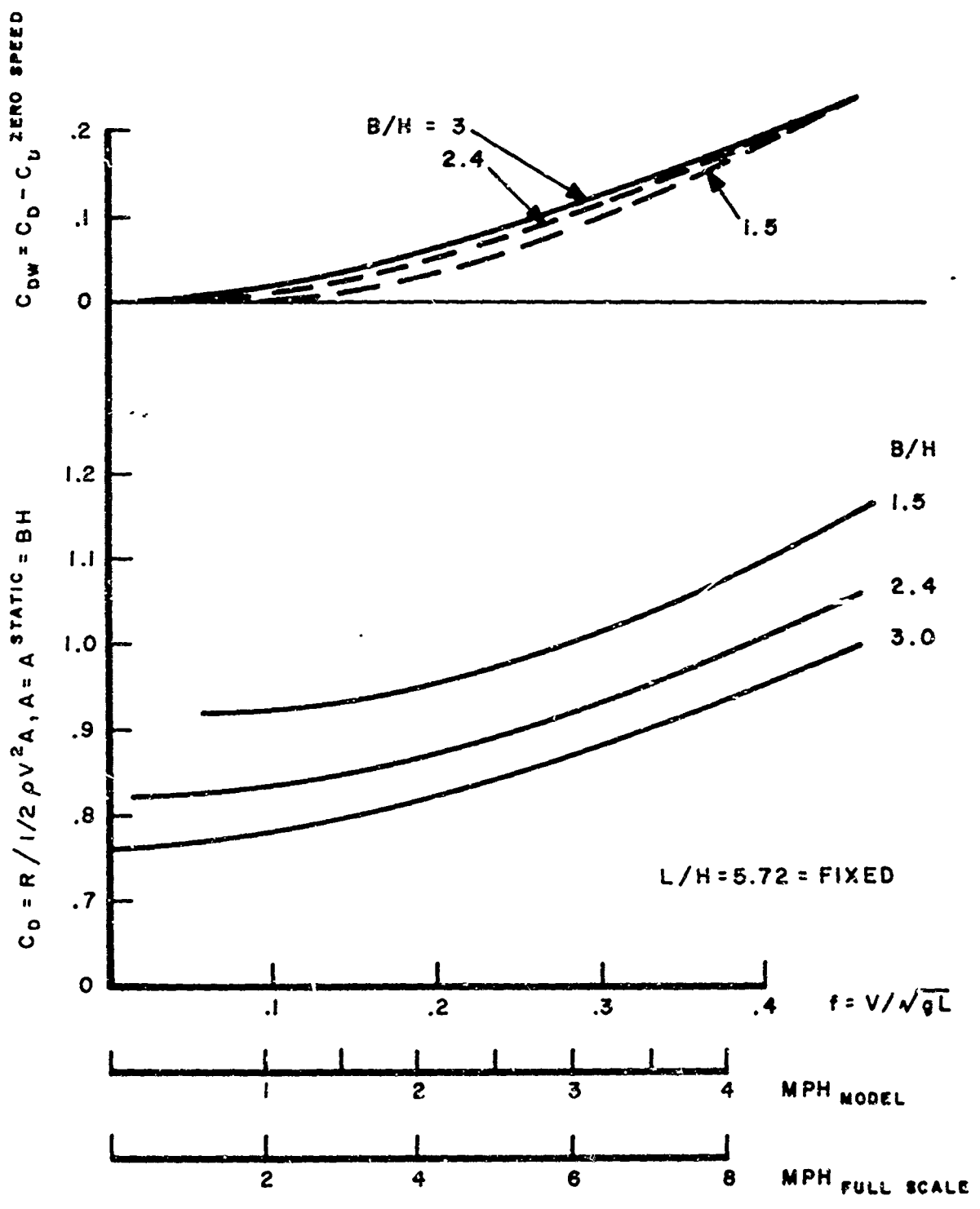
Figure 3.1A

Resistance Coefficients of Blocks as a Function of B/H,
For Various $v/\sqrt{gL}$, With L/H Fixed.
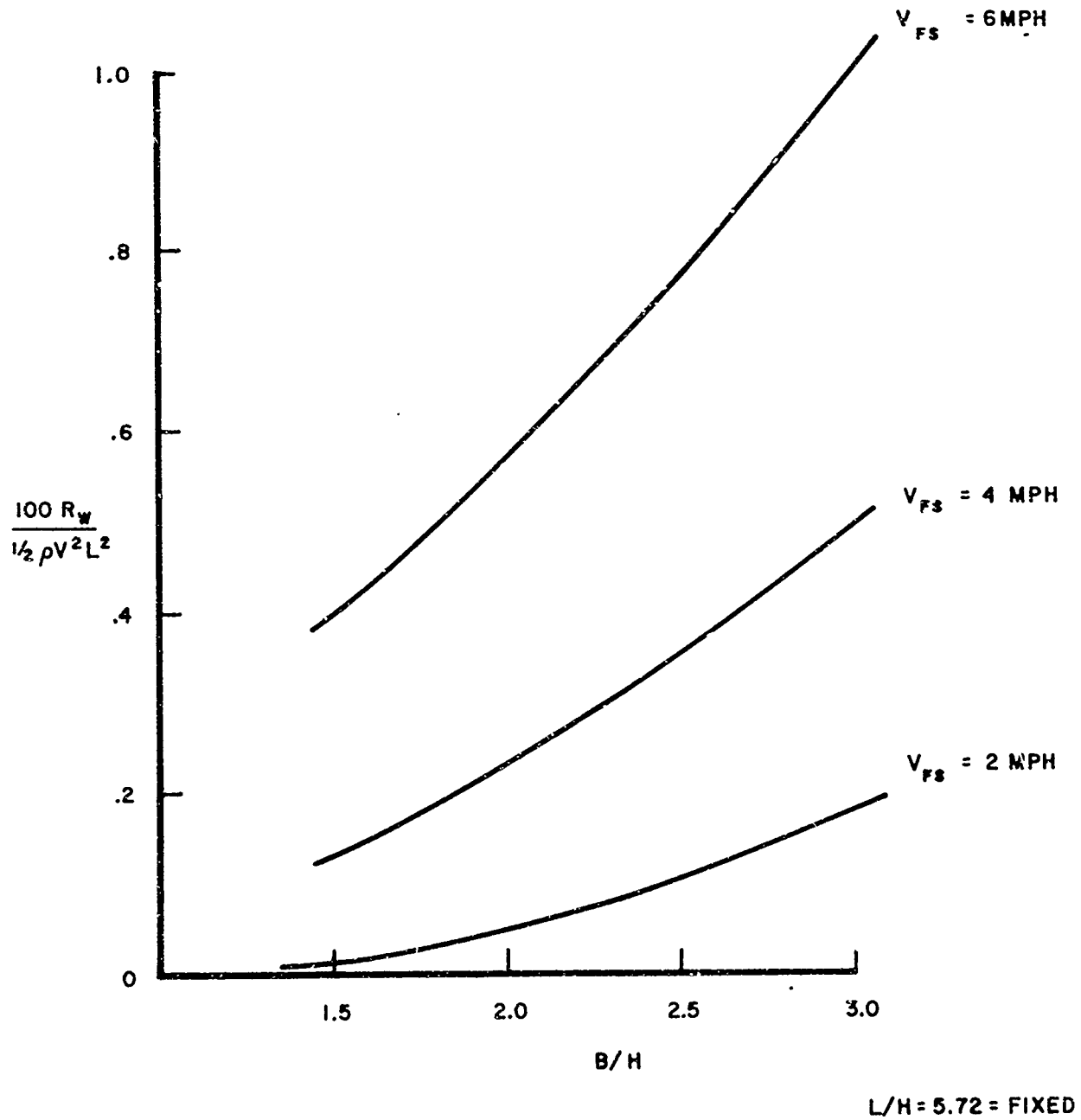
Figure 3.1b

$100\ R_W/\frac{1}{2}\rho v^2 L^2$ As a Function of B/H,

For Various $v/\sqrt{gL}$, With L/H Fixed.

The value of $A/2L^2$, a quantity which appears in the calculations, was

$$A/2L^2 = \frac{\rho g \forall}{2HL^2 \rho g} = .142$$

In the first set of calculations the model was represented by a constant-strength volume distribution of horizontal dipoles. The region occupied by the dipoles was a box. The length L_D and draft H_D of the box were fixed equal to the model length and model draft H, while the beam B_D of the box was varied (the subscript D denotes dipole). The constant strength was chosen to make linearized volume equal to model X-100 volume.

Case 1: Box length = model length

Box beam = 0 (Centerplane distribution, Michell theory)

Case 2: Box length = model length

Box beam = 1/2 model beam, $\beta = B_D/2L = .1$

Case 3: Box length = model length

Box beam = model beam, $\beta = .2$

These three calculations show the effect of spreading the dipoles laterally. The next set of calculations were the same except that the stern waves were eliminated by extending the model to infinity downstream. A possible justification for this is that the X-100 is blunt and has a strong wake, so that stern wave generation is small.

Case 4: Box length = semi-infinite downstream

Box beam = 0

Case 5: Box length = semi-infinite downstream

Box beam = 1/2 model beam, $\beta = .1$

Case 6: Box length = semi-infinite downstream

Box beam = model beam, β = .2.

The resulting <u>wave resistance</u> in pounds is plotted in Figure 3.2, together with the <u>total resistance</u> from model tests.

The calculated results for Cases 1, 2, 3 are much too high, and also display oscillations not present in the measured data. The calculated results do decrease as the distribution is spread laterally, as a result of increased wave interference. The calculated results for Cases 4, 5, 6 show that by eliminating stern waves we have reduced the mean resistance and eliminated the oscillations, as expected. Also, resistance again decreases as the distribution is spread laterally. Nevertheless, the numerical values of the calculated wave resistance are still too high, even for β = .2. Also, comparing against total measured resistance the trend at high speed appears wrong.

When we examine calculated wave resistance coefficients the picture darkens somewhat   (Figure 3.3). First of all there are the inevitable problems at very low speed. For β = 0 the calculated resistance coefficients approach non-zero constants as the Froude number goes to zero, the limiting value being twice as great with stern waves as without. If $\beta > 0$, the resistance coefficient vanishes like f^4 as $f \to 0$. Also, the calculated coefficients are too high and have the wrong trend at high speed.

The six dipole distributions tried above are quite rough. In the course of studying the flows generated by them (see Section 4) it was found that it is not a good idea to spread the distribution too much laterally since after some spreading the flow no longer generates a closed body. While it may turn out that resistance can be calculated with useful accuracy using
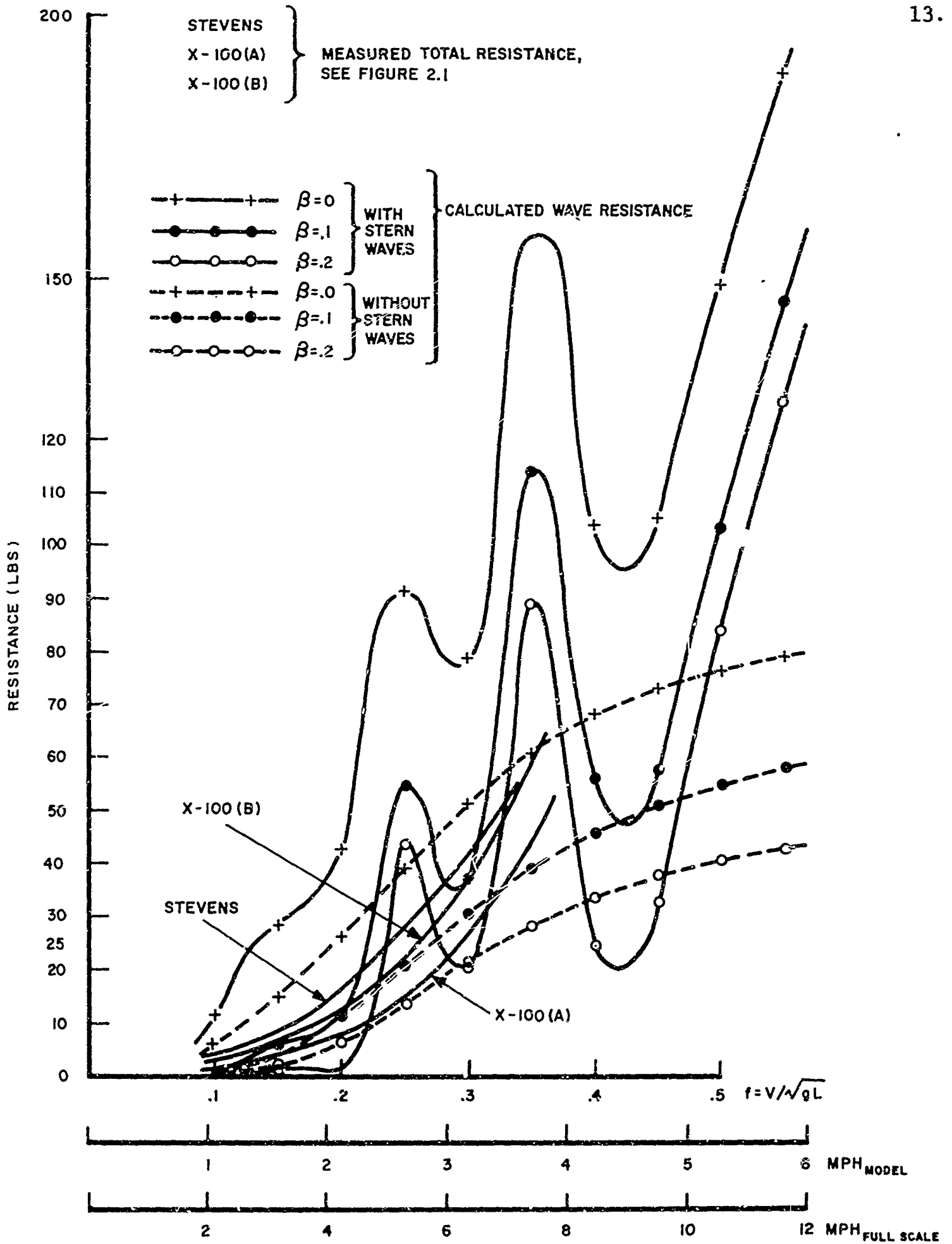
Figure 3.2

Various Measured Total Resistances and Calculated
Wave Resistances for LVTP5 Models
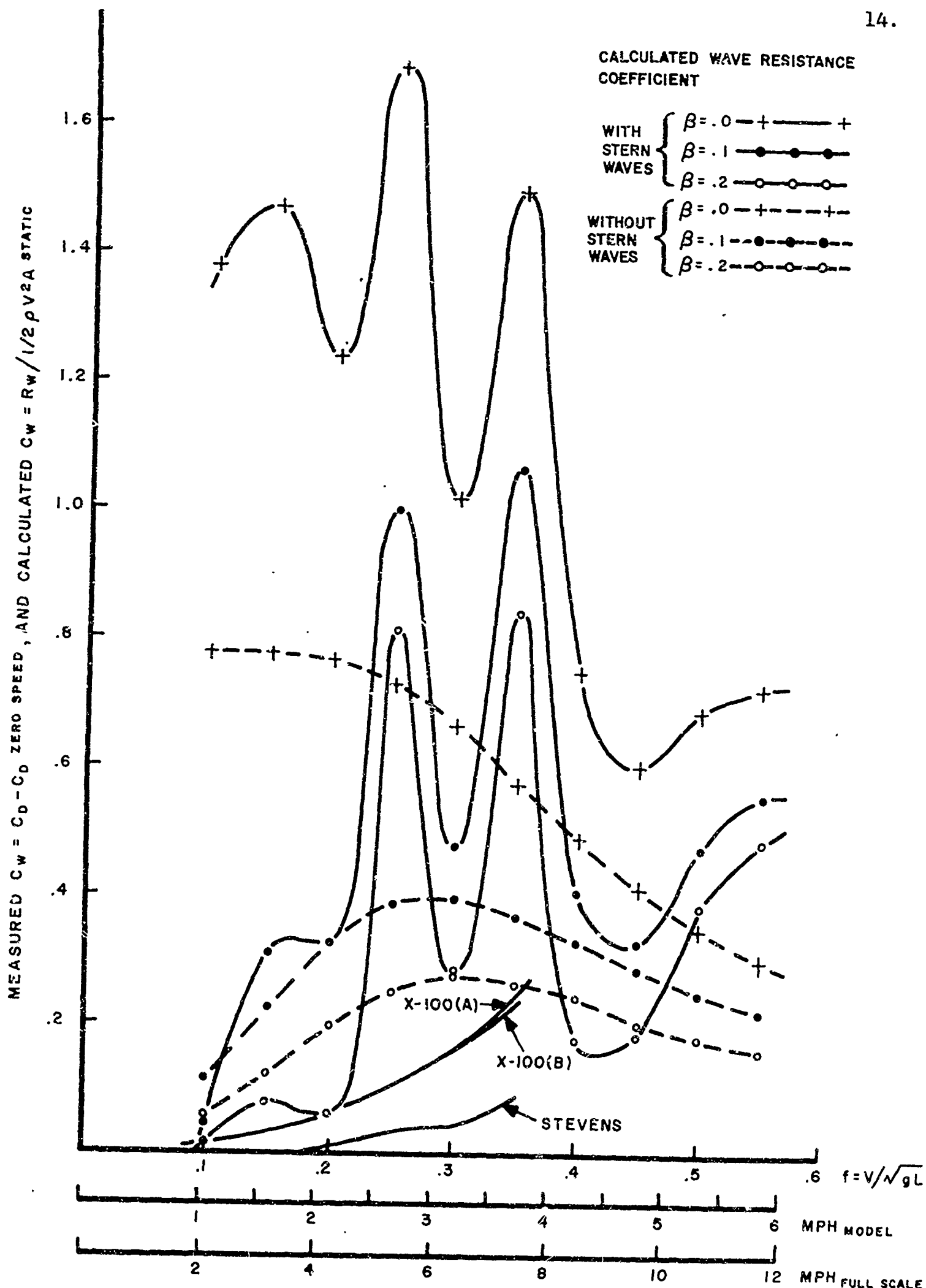
Figure 3.3
Various Measured and Calculated Wave Resistance
Coefficients for LVTP5 Models

4.

distributions which almost or approximately generate a closed
body we prefer not to pursue this approach till we know more
about it, especially since the functional form
$(f(x,y,z) = $ constant in a box) of the dipole distribution is
itself a gross approximation.

In Section 4 we say how we have used the Douglas Program
[3] to calculate the flow past an LVTP5 model. Part of the
Douglas Program output, namely the quadrilateral descriptions
and source strengths, can be used as inputs to our wave resistance
program. Wave resistance calculations of this type are described
in Section 5.

$\frac{1}{\sqrt{gL}}$

:L

SCALE

4. STREAMLINE CALCULATIONS FOR LVTP5 MODEL

4.1 Preliminary Discussion

Among the simple dipole distributions which are candidates for representing the LVTP5 model are those defined by functions

$$f_D(x,y,z) = f_D(x)g(y,z) \qquad (4.1)$$

where

$$f_D(x) = 1 \text{ for } |x| \leq \frac{1}{2}$$
$$= 0 \text{ elsewhere} \qquad (A)$$

or

$$f_D(x) = 1 \quad \text{for} \quad x \leq \frac{1}{2}$$
$$= 0 \text{ elsewhere} \qquad (B)$$

while

$$g(y,z) = \text{constant if } y,z \text{ in the region } A_S \text{ in the}$$
$$\text{yz-plane}$$
$$= 0 \text{ elsewhere.}$$

(A) represents a model of finite length, whose stern waves are undiminished by the wake. (B) represents a semi-infinite body having no stern waves. The product form (4.1) implies that the body will tend to have constant vertical sections except near its ends. The form of this vertical section depends on the region A_S and the function $g(y,z)$. A completely equivalent description is via a source distribution

$$f_S(x,y,z) = [\delta(x - \frac{1}{2}) - \delta(x + \frac{1}{2})]g(y,z) \qquad (A)$$

or

$$f_S(x,y,z) = \delta(x - \frac{1}{2}) \, g(y,z) \qquad (B)$$

where g(y,z) is as above and δ(x) is the Dirac δ-function.

We have evaluated resistance using both (A) and (B), and discussed the results in Section 3. We now consider the choice of suitable regions A_S and functions g(y,z) so as to approximate the LVTP5 model. Since the dipole distributions introduced above are too simple to represent the details of the LVTP5 model we introduce an equivalent box by requiring

$$L^E = L = 7.5' \qquad \text{(E denotes equivalent)}$$
$$B^E/H^E = B/H = 2.40$$
$$V^E = V = L^E B^E H^E = 20 \text{ ft.}^3$$
$$B^E = 2.530$$
$$H^E = 1.054.$$

The equivalent box has the same length, beam/draft ratio and displacement as the LVTP5 model.

A box-like dipole distribution is appropriate to approximate a box-like body, so we choose the region A_S to be a rectangle. We intend to compute the body from the dipole distribution, using the streamlines of the zero-speed flow (i.e. the flow satisfying $\partial\phi/\partial z = 0$ on the free surface). In effect this gives us the double body (body plus image in the free surface). Keeping this in mind we are led to an interesting constraint on the choice of the rectangle A_S on which a constant-strength source distribution is to be placed. Considering the sternless or semi-infinite situtation, the time rate of fluid addition is $4\pi\sigma_S A_S$ and far

downstream where the flow speed is unity the area A_∞ required
to transmit this fluid is

$$A_\infty = 4\pi\sigma_S A_S$$

There are two flow possibilities depending on the value of
$\sigma_S = \frac{1}{4\pi} (A_\infty/A_S)$, as shown in Figure 4.1. The x-velocity u_+ on
the upstream face of A_S is given by

$$u_+ = 2\pi\sigma_S$$

If $u_+ = 2\pi\sigma_S < 1$ then at every point in space the total x-velocity
is downstream, and there is no stagnation point or closed body.
If $u_+ = 2\pi\sigma_S > 1$ then there is a stagnation point and a closed
body, since the total x-velocity on the upstream face of A_S is
upstream. Hence

$$2\pi\sigma_S > 1$$

or

$$A_\infty > 2A_S$$

is a necessary and sufficient condition for the generation of a
closed body (ignoring the border line case $2\pi\sigma_S = 1$). This means
that if we wish to approximate the flow past an LVTP5 model
(with or without stern) by a flow of the type constructed above,
and with the approximate flow to generate a closed body, then
approximately we must require $A_S < \frac{1}{2} A_\infty$, where for A_∞ we use the
LVTP5 cross-section area at the central station. Recalling the
resistance calculations of the previous section, $\beta = .2$ would
mean that no closed body is generated, while $\beta = .1$ is borderline.
As stated elsewhere, the requirement that a closed body be
generated may not be mandatory.

INCIDENT FLOW
HAVING UNIT SPEED

Z

Y

X

$A_\infty = 4 \pi \sigma_s A_s$

$A_s =$ AREA OF RECTANGLE
CARRYING SOURCE
DENSITY σ_s
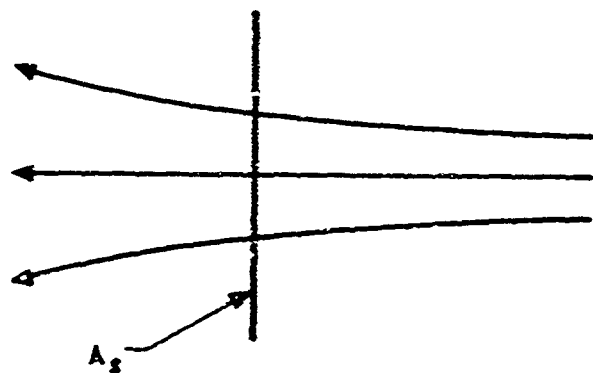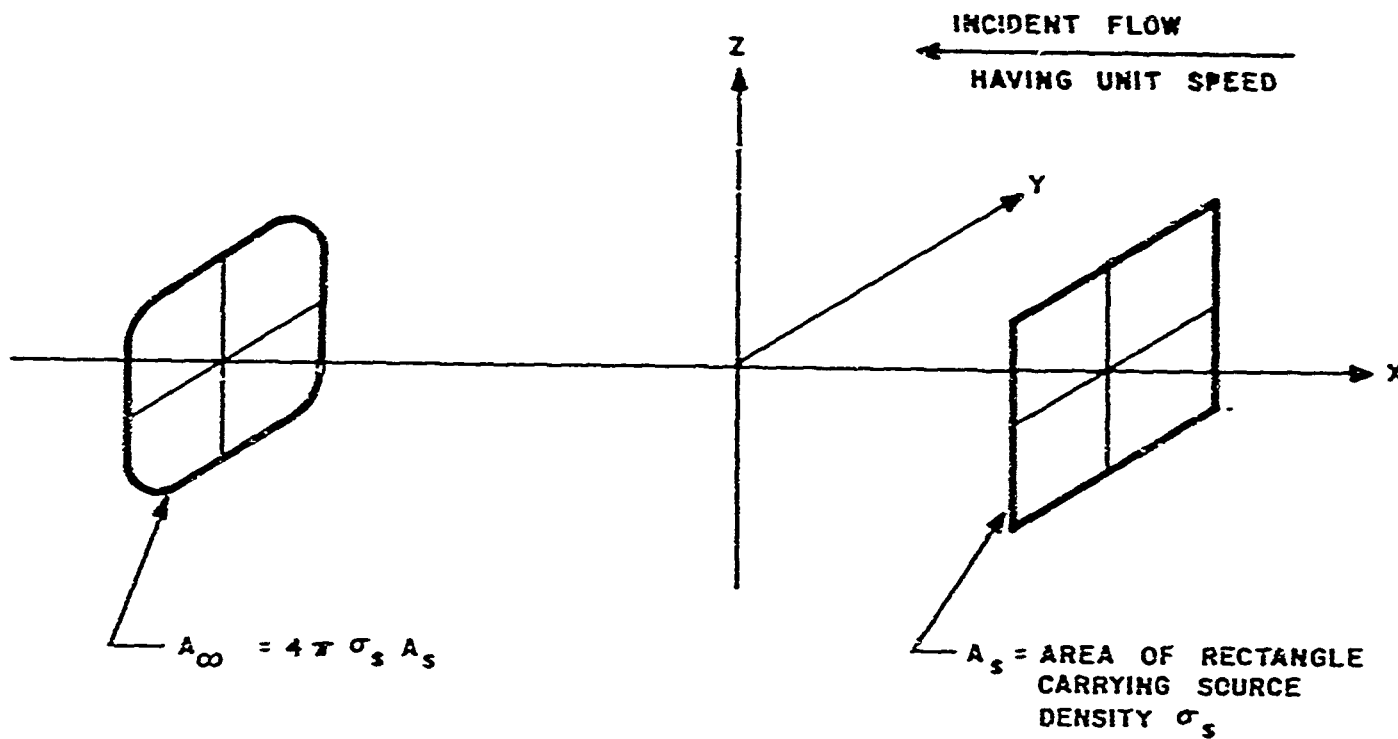
$u_+ = 2 \pi \sigma_s < 1$, NO STAGNATION POINT,
NO CLOSED BODY.

A_s

2 - DIMENSIONAL SKETCH ILLUSTRATING
3 - DIMENSIONAL SITUATION
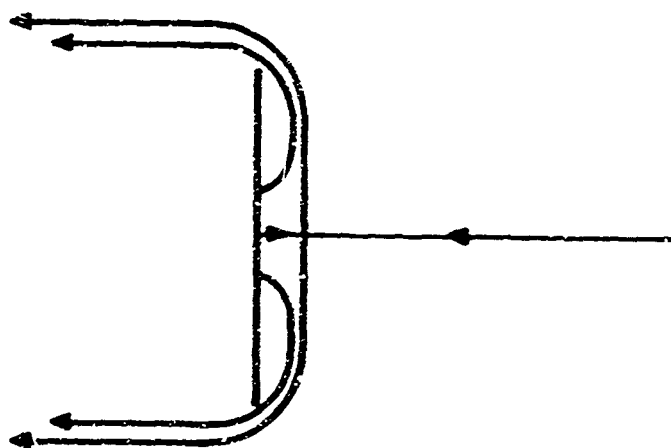
$u_+ = 2 \pi \sigma_s > 1$, STAGNATION
POINT, CLOSED BODY.

Figure 4.1
Possible Flows Generated by a Constant
Source Density on a Rectangle Normal
to a Uniform Flow.

We have calculated some streamlines of flow past a normal rectangular source sheet, as described above, which generated a closed body. They are described below in Section 4.2. In addition, surface source distributions were obtained for box-like bodies approximating, in two steps, the LVTP5 vehicle configuration. These are described in Sections 4.3 and 4.4.

4.2 Normal Rectangular Source Sheet

We have run some streamlines which confirm that if $2\pi\sigma_S < 1$ no closed body is generated. For illustration we show some streamlines for a case in which there is a closed body. The bow rectangle A_S is at $x = 0.5$ and is defined by $|y| \leq .113$, $|z| \leq .0942$, $A_S = 0.01065$. We have $\sigma_S = 0.177$, so that $A_\infty = 2.22\ A_S$. The stagnation point was found at $x = + 0.5116278$. Figure 4.2 shows the y-z projections of streamlines starting at this value of x and at a distance of 0.001 from the x-axis at various indicated angles from the y-axis. It shows that all such body streamlines are tangent to the x-y plane at $y = 0.0$. Figure 4.3 shows sections through the half-body generated at various values of x.

-z

4.3 Simple LVTP5

A simplified body close in shape to the LVTP5 was drawn up. The surface was divided into 59 quadrilaterals of about uniform area (for 1/4 of the submerged body) and the constant source strength over each quadrilateral was found (via the Douglas Program [3]) which satisfied the boundary condition at
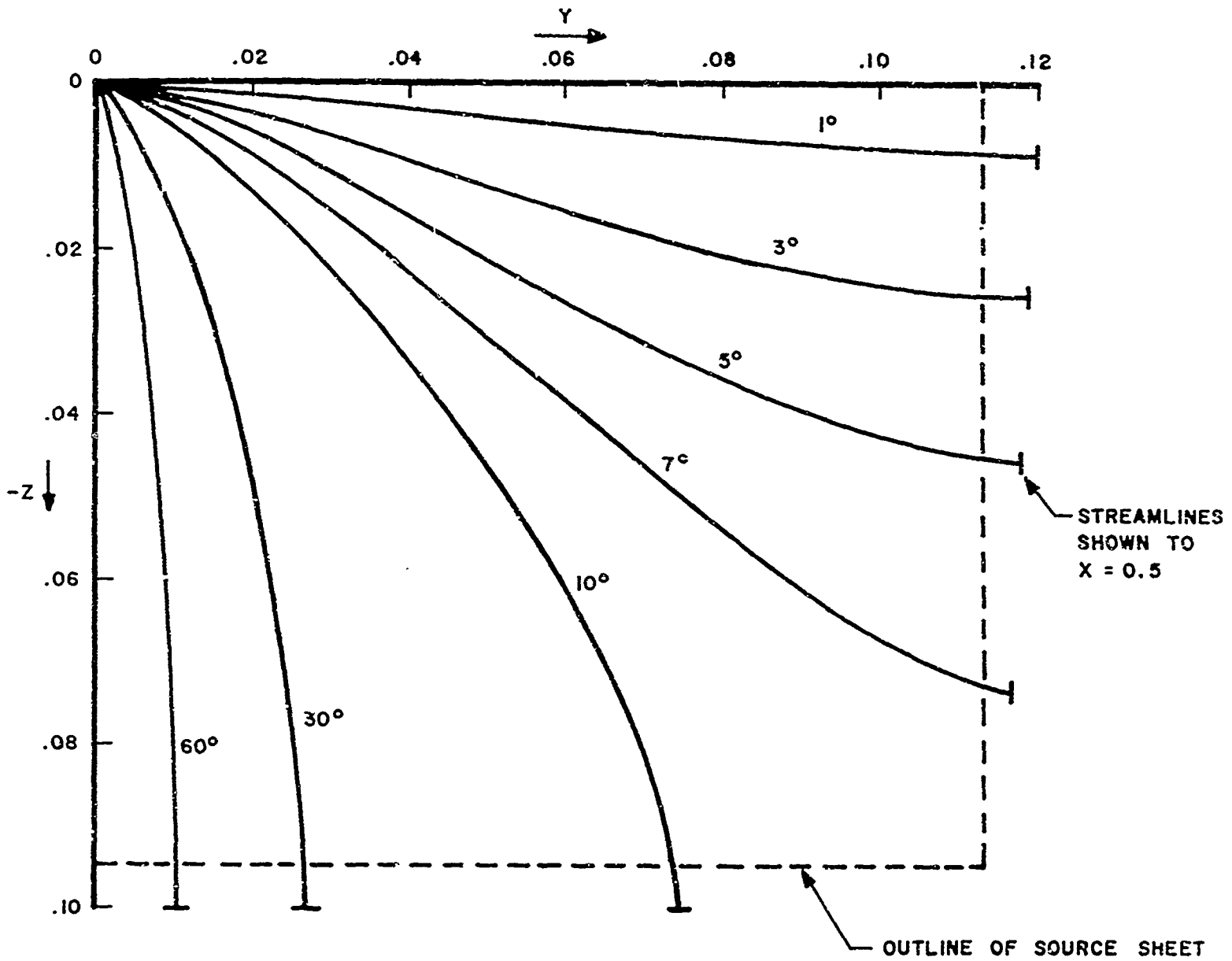
ALL STARTING POINTS AT X = .5116278 AND .001 FROM X - AXIS.
ANGLE INDICATED IS THAT OF STARTING POINT FROM Y — AXIS

Figure 4.2

yτ-Projections of Streamlines Generated
by a Constant Source Density on a
Rectangle Normal to a Uniform Flow.
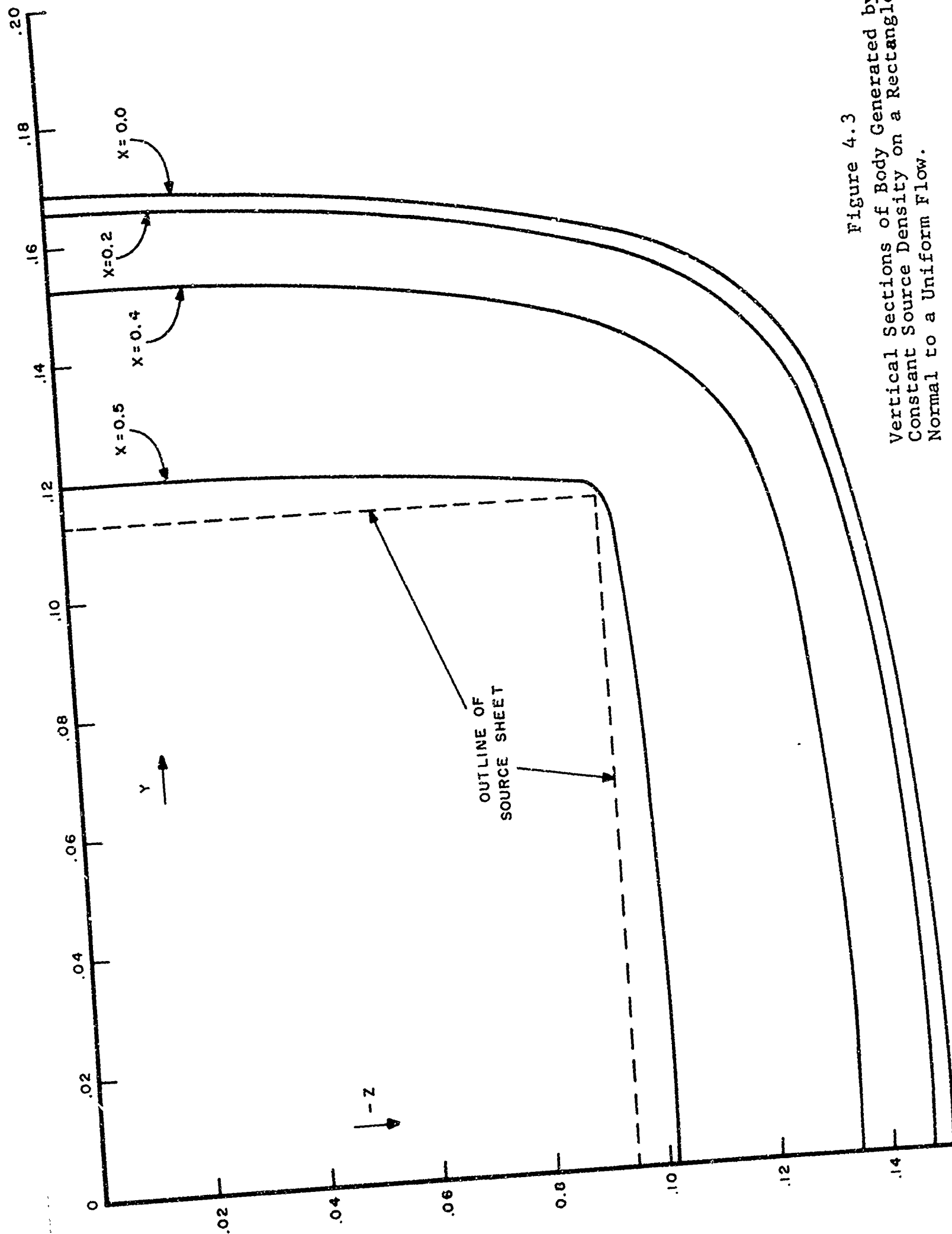
Figure 4.3

Vertical Sections of Body Generated by a
Constant Source Density on a Rectangle
Normal to a Uniform Flow.

22.

one point on each quadrilateral. Using a Douglas Program Post
Processing Program developed by TRG, and TRG's Streamline Program,
various streamlines were calculated for the resulting singularity
distribution. These streamlines were poor approximations to the
true flow field in that they passed through the body. This was
caused by negative sources on the front of the body. These
negative sources are thought to be the erroneous result caused
by using too few quadrilateral elements to approximate the body
surface. These results indicated the nature of the refinement
necessary to obtain reasonable streamlines from approximate
surface singularity distributions determined using the Douglas
program and our programs.

4.4 TRG LVTP5 Model

A surface singularity distribution was calculated for
the LVTP5 hull shape (with the tracks and wheels removed and the
well filled in). Figure 4.4 shows the assumed body surface
which was divided into 223 quadrilaterals (over 1/4 of the sub-
merged body). The quadrilaterals were smaller in the bow region
than towards amidships. The Douglas Program was applied to this
input body surface and calculated the source strength for each
quadrilateral element, uniform over each element, which satisfied
the boundary condition at one point on each element. This
singularity distribution was used to calculate the streamlines
of the flow. A saddle stagnation point (see Reference [4]) was
found on the x-axis at x = 14.230". This type of stagnation point
is believed to be due to the indented V-bow. Figures 4.5 and 4.6
show the x-y and x-z projection respectively of various calculated

Normal to a Uniform Flow.
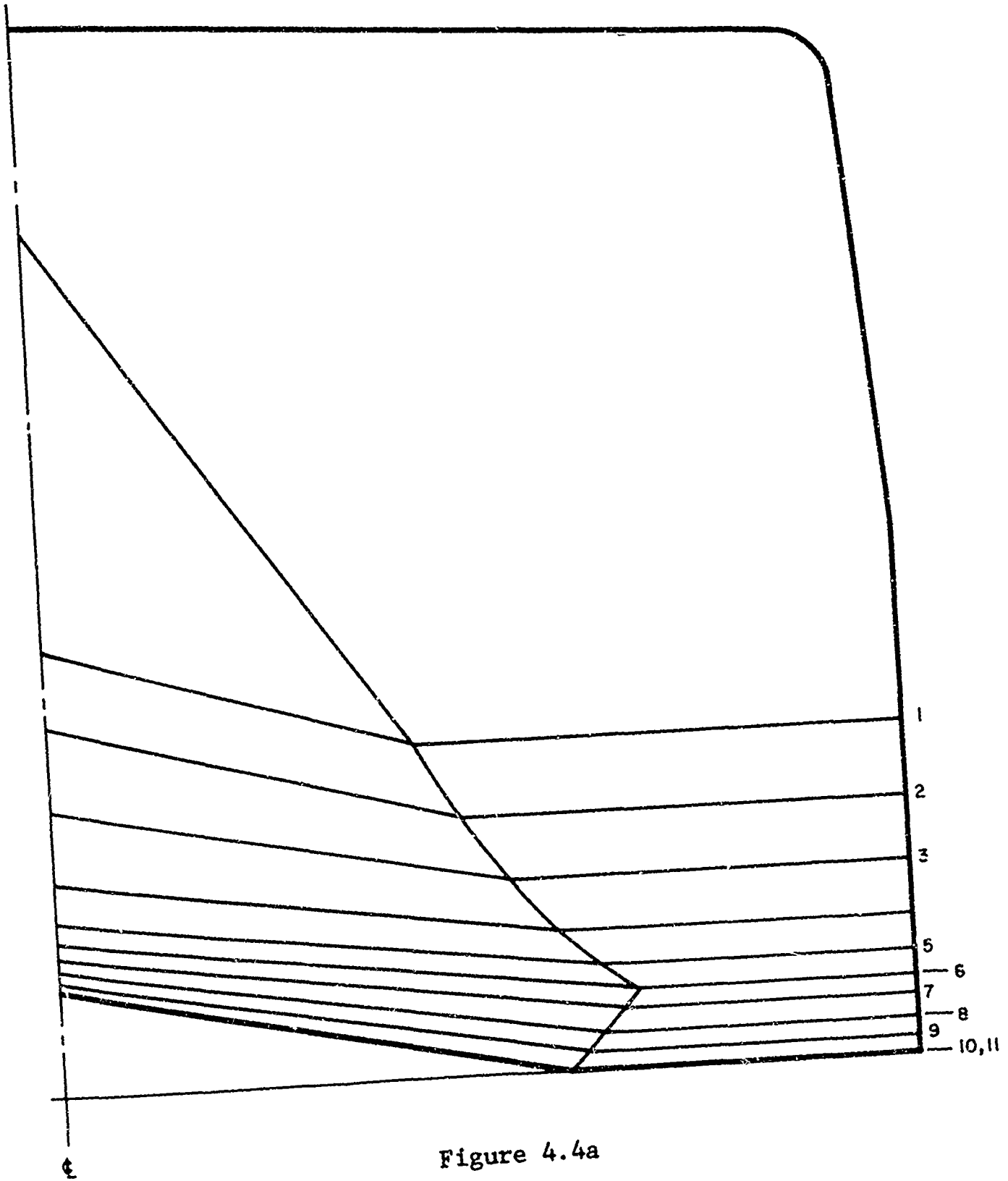
Figure 4.4a

LVTP5 Body Surface used for
Streamline Calculations, Body Plan.
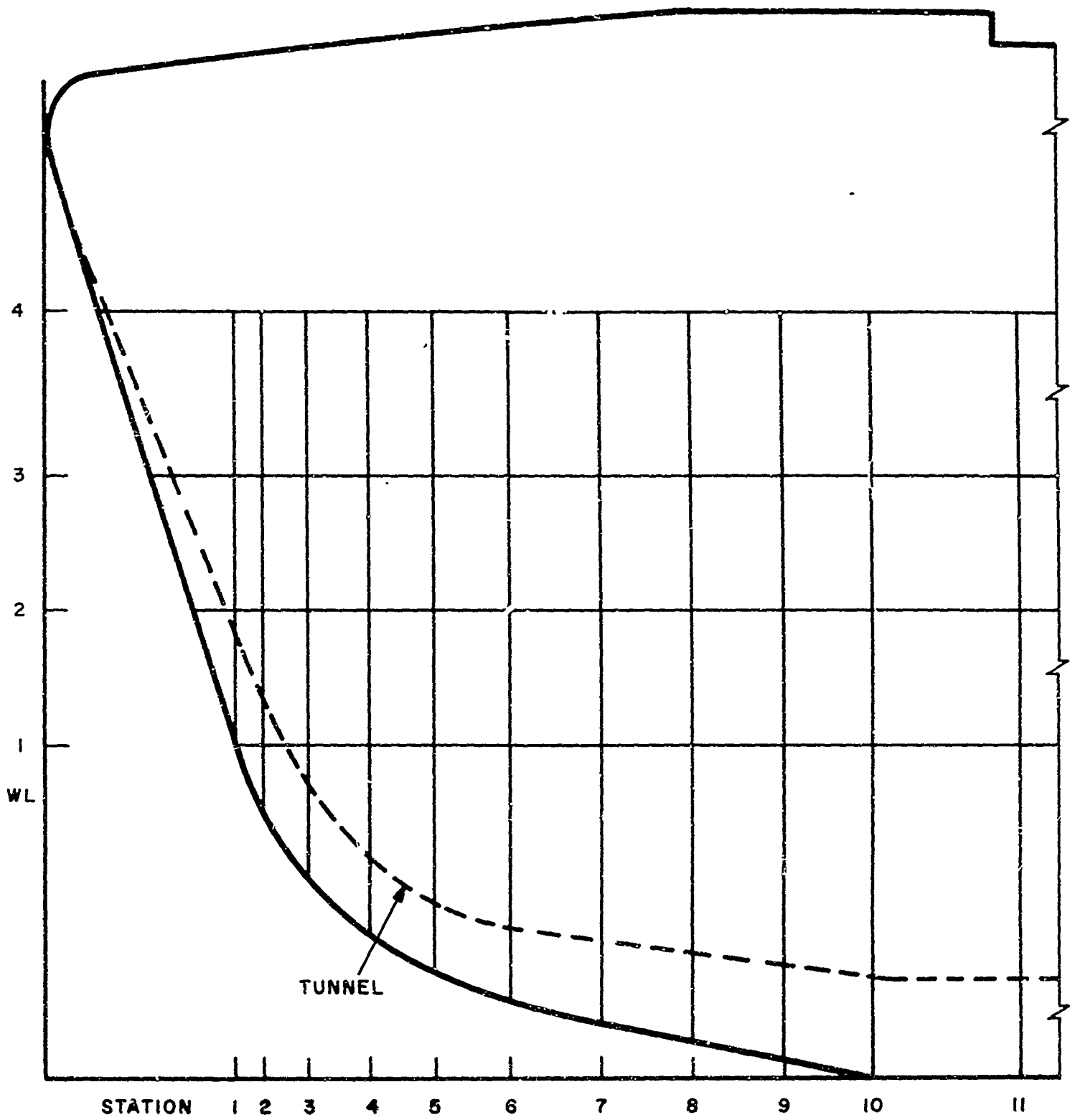
Figure 4.4b

LVTP5 Body Surface used for
Streamline Calculations, Profile
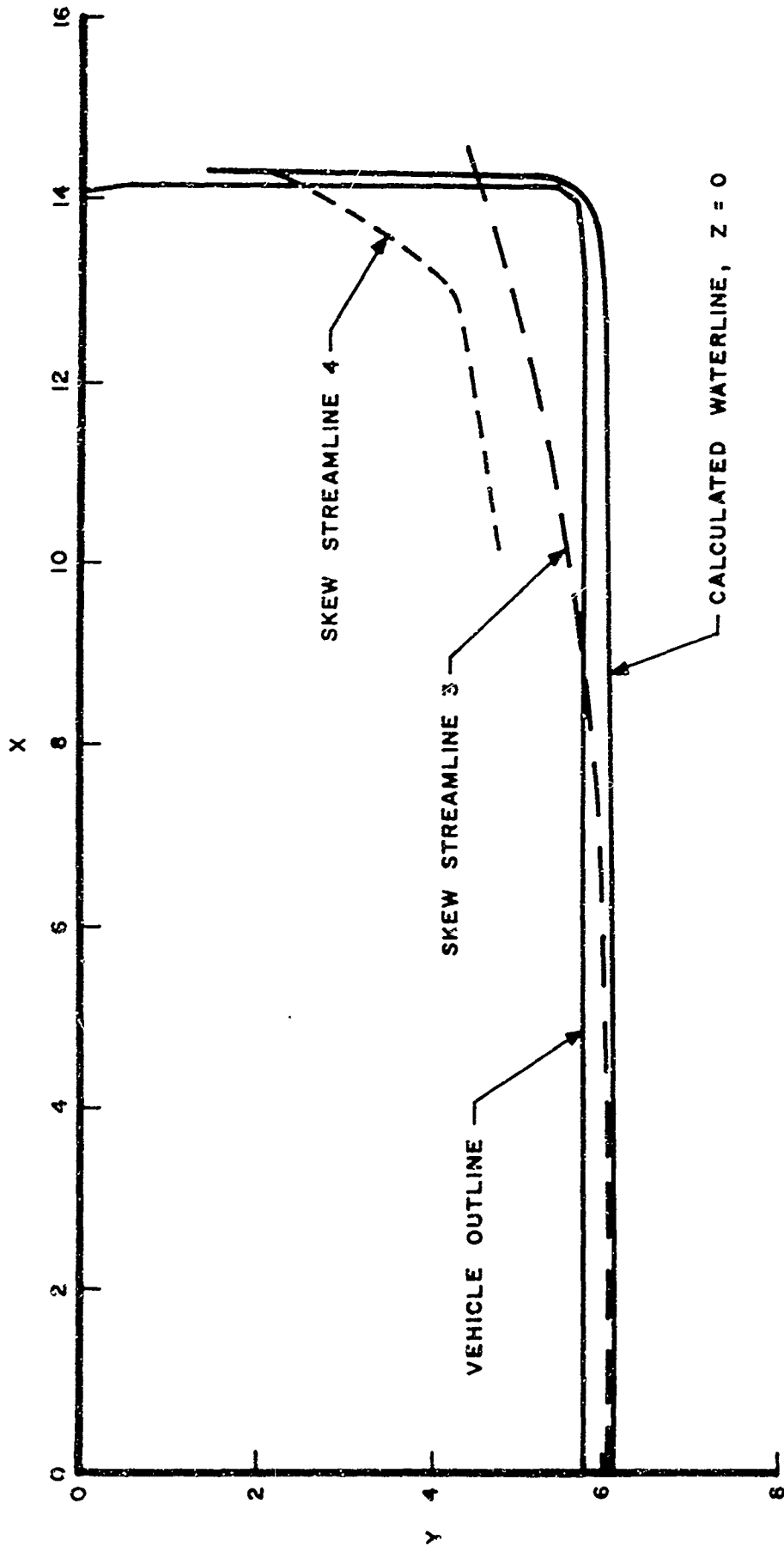
Figure 4.5

xy-Projections of Various Calculated
Streamlines of Flow Past LVTP5 Model
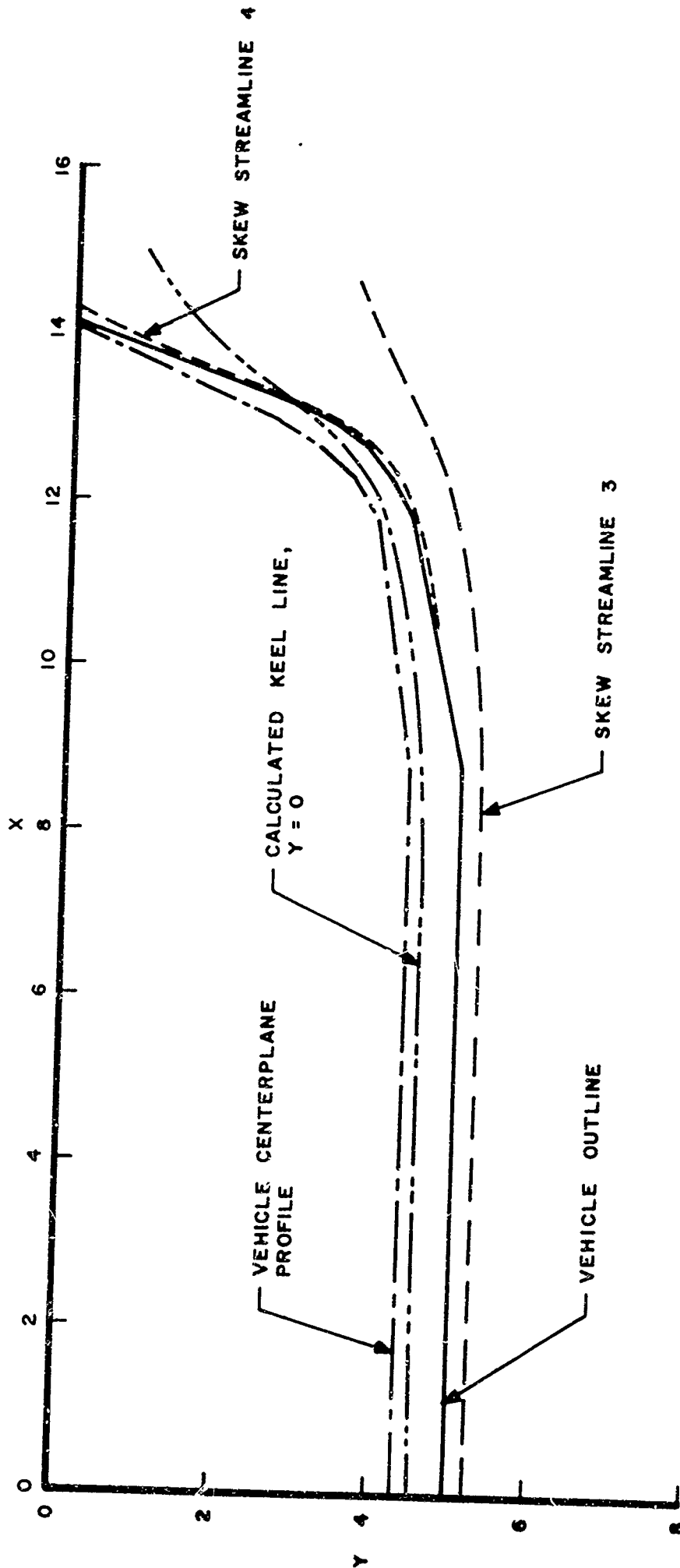
Figure 4.6

xz-Projections of Various Calculated

Streamlines of Flow Past LVTP5 Model

streamlines in relation to the LVTP5 body surface. Here it is seen that streamlines very close to the body, such as the waterline or keel line, can be obtained without difficulty. The skew streamlines, which are also very close to the body surface, indicate the predominant lateral flow on the bow ramp of the vehicle. Since the streamlines for the generated singularity distribution are reasonable, a calculation of linearized volume was made based on the resulting 223 source strengths. The result is a linearized volume of 447 cubic inches (per 1/4 of submerged model). The actual volume is 395 cubic inches. This ratio of linearized to actual volume (447/395 = 1.13) is about what we expect, based on the known relation between true volume, linearized volume or dipole moment, and added mass in the forward direction, and is a partial check on the accuracy of the calculation of the source strengths.*

A sample of computer input data and a sample of computer output, for streamline calculations, is given on the following two pages.

---

* Previous experience with shiplike forms generated by singularity distributions also indicates that a ratio of 1.13 is reasonable.

STARTING POINT X= 14.23 Y= 0.1   Z= 0.0
INITIAL STEP-SIZE =   1.0
J   EXIT WHEN X(1   )
FACT IS LESS THAN   (-1.0   )
YMAX   IS 0.0
MAXIMUM NUMBER OF POINTS PER STREAMLINE =   5
PRINT ON-LINE AFTER EACH 13   POINTS
UPPER BOUNDS ON TRUNCATION ERROR , U1=   0.05 , U2=   0.0
LOWER   BOUNDS ON TRUNCATION ERROR , L1=   0.005   L2=   0.0
INPUT NEW BODY DESCRIPTION
PERFORM INTERPOLATIONS
THERE ARE 7 X-STATIONS
LOCATED AT X= 14.14 12.726 11.312 8.484 5.656 2.828 0.0
THIS BODY CONSISTS OF 6 STREAMLINES
SCALE FACTOR FOR COORDINATES IS 12.0
*   BODY DESCRIPTION
ONSET FLOW COMPONENTS ARE VX= 1.0   , VY=   0.0   , VZ=   0.0
PROXIMITY CRITERIA ,   RHO1= 2.45   ,   RHOZ2=   4.00
PLANES OF SYMMETRY =   3
NUMBER OF BASIC ELE MENTS = 223

SKEW LINE 4   DOUGLAS PROGRAM CASE 12 - 10/15/65

STARTING POINT X= 14.3 Y= 2.0 Z= 0.01
INITIAL STEP-SIZE =   1.0
FACT   -1.0
YMAX   0.0

X	Y	Z	U	V	W	$1-(V/VINF)^2$	STEP-SIZE	TRUNC. ERR.
1.4300000E 01	2.0000000E 00	9.9999999E-03	-1.4503302E-02	1.0646513E-01	8.3125435E-03	9.8838573E-01	1.00000E 00	0.
1.4299305E 01	2.1106242E 00	2.3557972E-02	-7.1214546E-03	1.1456079E-01	2.0690609E-02	9.8632528E-01	1.00000E 00	1.72508E-03
1.4251444E 01	2.2577333E 00	1.2962395E-01	-2.9061817E-02	1.3240491E-01	1.0599400E-01	9.7039962E-01	2.00000E 00	3.00593E-02
1.4212440E 01	2.4950681E 00	2.6850590E-01	-7.9292240E-02	1.4262258E-01	1.6884030E-01	9.4486352E-01	1.00000E 00	1.48119E-02
1.4110374E 01	2.5434895E 00	4.5345950E-01	-1.1741848E-01	1.5432728E-01	1.9277498E-01	9.2523379E-01	1.00000E 00	2.01650E-02
1.4079042E 01	2.9042820E 00	6.5235965E-01	-4.3442951E-02	1.6857795E-01	2.3036033E-01	9.1552847E-01	1.00000E 00	3.87250E-02
1.3911543E 01	2.9829372E 00	9.1573130E-01	-1.1233129E-01	1.4923617E-01	2.8772126E-01	8.6878783E-01	1.00000E 00	1.73804E-02
1.3749326E 01	3.1937222E 00	1.2237250E 00	-1.2180471E-01	2.1271158E-01	3.4683643E-01	8.1962091E-01	1.00000E 00	3.05871E-02
1.3505456E 01	3.4089361E 00	1.5953238E 00	-1.4154651E-01	2.3801444E-01	4.0092586E-01	7.6250787E-01	1.00000E 00	1.74767E-02
1.3503004E 01	3.5598315E 00	2.0325851E 00	-1.7085533E-01	2.6364719E-01	4.7480562E-01	6.7285786E-01	1.00000E 00	1.04791E-02
1.3392056E 01	3.7346264E 00	2.5578532E 00	-2.1324512E-01	2.8415967E-01	5.8199933E-01	5.3517253E-01	1.00000E 00	4.59201E-03
1.3133376E 01	4.0773811E 00	2.8763160E 00	-3.0526274E-01	2.8386339E-01	7.1588737E-01	3.1072847E-01	5.00000E-01	5.81366E-03
1.3112483E 01	4.1709936E 00	3.0599520E 00	-3.3251500E-01	2.7169111E-01	7.3535783E-01	2.7486657E-01	2.50000E-01	3.04126E-02
1.3295423E 01	4.2109522E 00	3.2526110E 00	-3.1790763E-01	2.3342856E-01	8.8090342E-01	6.8377629E-02	2.50000E-01	3.24934E-03
1.2731923E 01	4.2413002E 00	3.3771873E 00	-5.6952296E-01	2.5011063E-01	9.3564805E-01	-2.6234901E-01	1.25000E-01	2.44747E-03
1.2396523E 01	4.2728969E 00	3.4906210E 00	-6.1370043E-01	2.5947032E-01	8.9279950E-01	-2.4299235E-01	1.25000E-01	2.55621E-03
1.2727355E 01	4.3543705E 00	3.7210245E 00	-7.5928055E-01	2.5152754E-01	1.0145677E 00	-6.6760228E-01	2.50000E-01	4.58806E-04
1.2502272E 01	4.3793758E 00	3.7422268E 00	-9.8583766E-01	2.4013874E-01	8.1626649E-01	-6.9139463E-01	2.50000E-01	3.17697E-02
1.2235703E 01	4.4593766E 00	4.1422732E 00	-1.1788229E 00	2.2290849E-01	7.2987686E-01	-9.7203203E-01	2.50000E-01	1.35845E-02
1.1710403E 01	4.5099310E 00	4.3069786E 00	-1.2272342E 00	2.0217157E-01	6.2261555E-01	-9.3794613E-01	2.50000E-01	4.10397E-02
1.1915166E 01	4.5515135E 00	4.4336497E 00	-1.3069786E 00	2.0311766E-01	4.1058124E-01	-9.0067395E-01	2.50000E-01	2.87511E-02
1.1295167E 01	4.5116419E 00	4.5227635E 00	-1.3552005E 00	1.9787507E-01	2.4659407E-01	-9.8652162E-01	2.50000E-01	1.75414E-02
1.0759379E 01	4.5603158E 00	4.5619565E 00	-1.1752066E 00	1.9087790E-01	1.1021448E-01	-4.2969224E-01	2.50000E-01	2.10206E-02
1.0702119E 01	4.7059145E 00	4.5877090E 00	-9.3553097E-01	1.8203658E-01	1.4480280E-01	7.0676804E-01	2.50000E-01	2.10206E-02
1.0450377E 01	4.7511386E 00	4.6576676E 00	-1.0229119E 00	1.7093843E-01	3.4239915E-01	-1.9260128E-01	2.50000E-01	2.55456E-02

EXIT DUE TO MAXIMUM NO. OF POINTS

5. DOUGLAS RESISTANCE CALCULATIONS

The application of the Douglas Program to the idealized LVTP5 was described in Section 4. The resulting source distribution has a wave resistance which can be calculated using the point source approximation, in which each quadrilateral carrying constant source strength is replaced by a point source (having the same total strength) at its centroid. We calculated the wave resistance in this way, without stern waves. The result is plotted in Figure 5.1. At full-scale speeds above about 3 MPH the calculated resistance rises rapidly and becomes about twice the block resistances (β = .0,.1,.2 in Figure 5.1). At low speeds this calculated resistance falls below the previous calculations for β = .0, .1. The high values can be explained on the basis of the factor of 2, discussed in Section 4, which relates the source density generating a stagnation point and the source density generating the proper volume. We expect to find the higher value $\sigma = \frac{1}{2\pi} = .159$, in the case of the Douglas output, near the bow of the vehicle, and inspection of the printed source strengths reveals that indeed the values of σ are in the range .13 - .17. According to this reasoning the Douglas resistance should be roughly four times the resistance plotted for β = .2 in Figure 5.1, and it is. At low speeds the sources over the sides and bottom of the vehicle, which are present in the Douglas calculation but not in the block calculations, cannot be neglected and the reasoning becomes incomplete.

STEVENS
X-100 (A) } MEASURED TOTAL RESISTANCE
X-100 (B)   SEE FIGURE 2.1

POINT SOURCE BASED ON DOUGLAS
$\beta = .2$ PLUS BULB
$\beta = .0$
$\beta = .1$
$\beta = .2$

CALCULATED WAVE RESISTANCE
WITHOUT STERN WAVES

RESISTANCE (LBS)

X = 100(B)

STEVENS

X = 100 (A)

BULB DESIGN SPEED

$f = V / \sqrt{gL}$
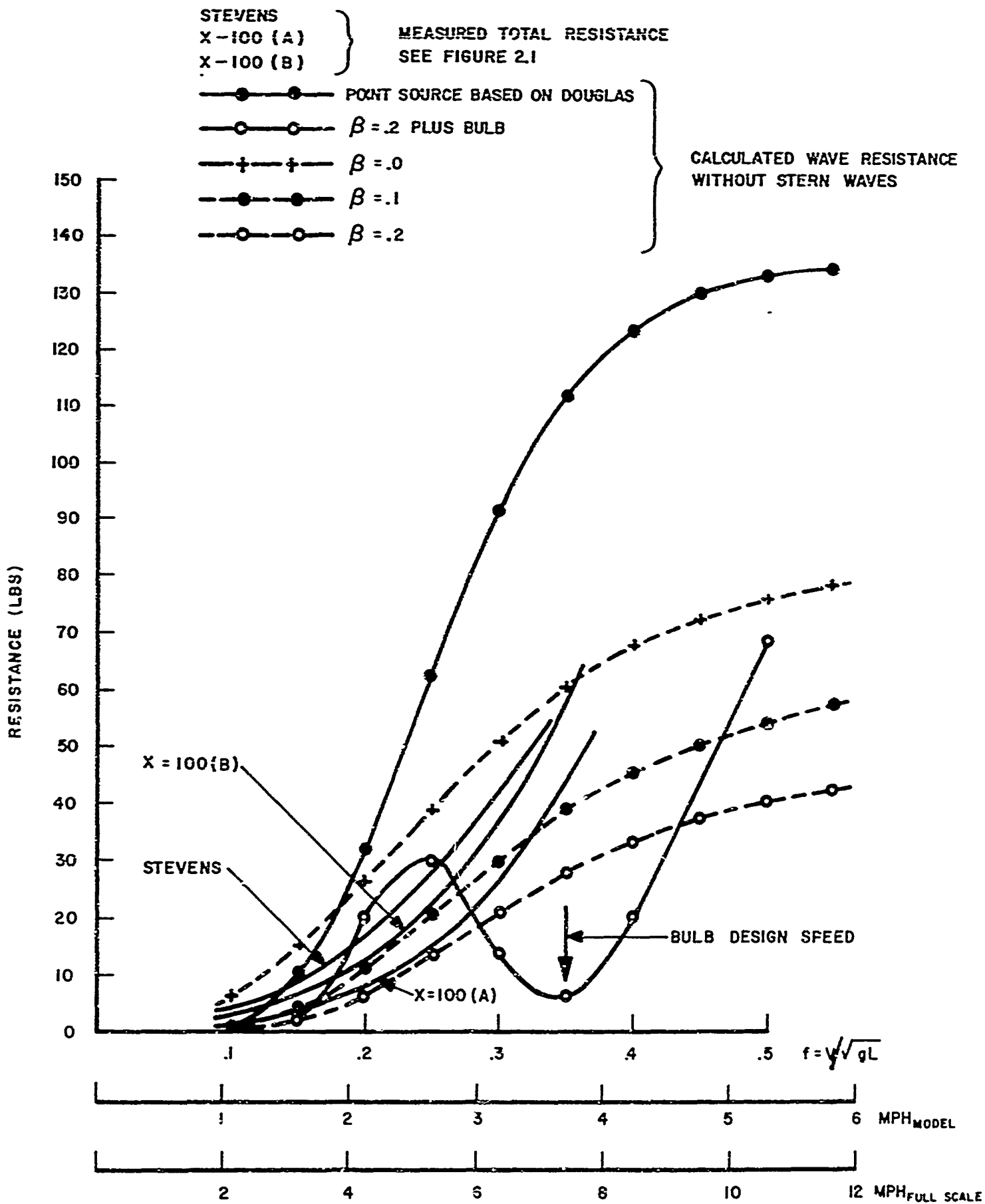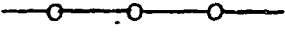
MPH$_{MODEL}$

MPH$_{FULL\ SCALE}$

Figure 5.1

Various Measured Total and
Calculated Wave Resistances for LVTP5 Models

On the basis of a comparison made on a Series 60 hull, for which wave resistance based on the Douglas Program was calculated exactly and using the point-source approximation, we believe that the point-source approximation is adequate except at the lowest speeds of interest. In view of the unpromising nature of the calculated results based on the point-source approximation, and the anticipated cost of the exact calculations, we decided not to make the exact calculations.

It appears that wave resistance calculations based on the Douglas Program do not provide useful results for the idealized LVTP5. One possible explanation is that wave velocities are not used in the Douglas program which determines the source strengths, so that the source strengths are not right. Another possible explanation is that a theory in which the free surface is linearized, even with the proper source strength, is not a useful approximation for bodies as blunt as the LVTP5.

The block resistance calculations give the best resistance predictions, even though they do not represent the shape of the hull as accurately as the Douglas source distribution does.

6. THE EFFECT OF HULL MODIFICATIONS ON RESISTANCE

Using the block model of the LVTP5 resistance we have considered bow modifications intended to reduce resistance. Not a great deal was done in this direction but some interesting results were obtained. In Figure 5.1 the curve —o—o—o— is calculated wave resistance without stern waves for the block representation of the LVTP5 (with β = .2), modified by a bulb. The bulb is generated by a horizontal line of horizontal dipoles, the dipole strength being given by a quadratic function of x whose coefficients were determined by digital optimization at a Froude number f = .35. We see that the calculated wave resistance is indeed reduced at f = .35, and also at other Froude numbers. The dipole distribution representing the bulb is rather wild, and we did not have time to verify that a closed body is in fact defined. If a closed body is not defined the next step would be to determine what resistance penalty is incurred by restricting the optimization to realistic dipole distributions. The large calculated resistance reduction suggests that the subject is worth pursuing.

7. CONCLUSIONS AND FUTURE WORK

The practical aims of the project are to produce new configurations which will have increased speed in the water. We have begun by seeking an improved theoretical understanding of the measured data obtained to date. Some points to be established are:

1) what fraction of the vehicle drag or power consumption is attributable to wave resistance,

2) what fraction of the vehicle drag or power consumption is attributable to poor flow to the foremost grousers.

Regarding 1) we have found (in Section 2) that the estimated wave resistance lies between 15% and 50% of the total resistance at full-scale speeds in the neighborhood of 7 MPH. This uncertainty is large. The total resistance is itself uncertain to the extent of some 30%. Regarding 2) we know from Figure 277 of [2] that at model displacements of 938 lbs. and 1095 lbs. the power requirements rise very sharply at model speeds of 3.3 and 3.25 MPH respectively, and this sharp rise is correlated with the appearance of a void at the vehicle shoulder and attendant poor flow to the leading grousers. At a model displacement of 1250 lbs. (80,000 lbs. full scale) this phenomenon occurs at a model speed of 3.9 MPH. For a model displacement of 1400 lbs. the power rises sharply at lower speeds for another reason, namely that the bow of the vehicle is completely covered with water at 3.25 model MPH. It is curious that for a 1250 lb. model the onset of poor flow to the grousers is not reflected in curves of nominal propulsive efficiency η, defined by

$$\eta = HP^{TOWING}/HP^{TRACK}$$

Figure 7.1 shows two curves of η based on HP^{TOW} with tracks running at zero slip and stationary, for 1250 lbs. model displacement. η rises steadily with the tracks at zero slip, and rises steadily but levels off at 3 model MPH with tracks stationary. With 938 lb. model displacement we find a sharp drop in nominal efficiency at a model speed of 3.2 MPH, which correlates well with the appearance of a shoulder void and a sharp rise in track horsepower at 3.3 MPH (see above).

We may summarize by saying that on the basis of data used in preparing this report neither of the questions 1), 2) above can be answered in a satisfactory way.

The nominal efficiency defined above differs from the efficiency based on the propulsive force exerted by the tracks on the model. Reference [2] states that the efficiency (undefined) is of the order of 10-13% using the best grousers. This is of the same order as what we show in Figure 7.1 but the data in [2] is less variable with speed.

Given the present vehicle as a starting point it is clear from Figure 7.1, in spite of the inaccuracy of the data, that there is more to be gained by improving propulsive efficiency than by reducing resistance. However, if propulsive efficiency is increased the relative importance of reducing resistance will increase. This increase in the importance of reducing resistance will be rapid since the top speed of the vehicle will increase
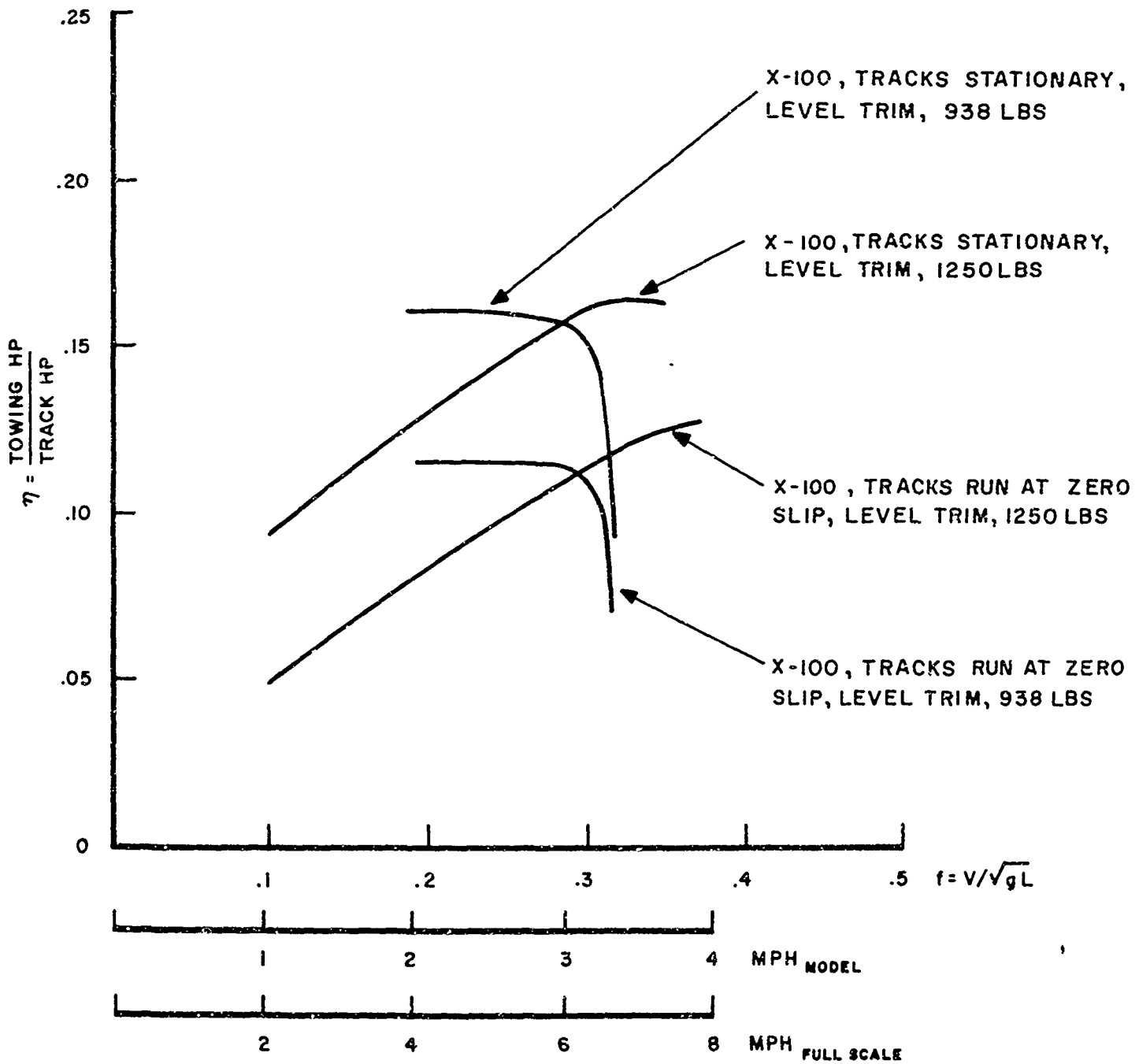
Figure 7.1

Nominal Propulsive Efficiencies of
Track-Propelled X-100 Model, 1250 lbs. and 938 lbs.
Model Displacement, Level Trim.

for constant installed power, and hence the drag will also
increase.

We believe that it would be appropriate to continue
our development of theoretical models of resistance and flow.
At the same time, the development and test of improved
configurations, following the bulb whose calculated performance
is shown in Figure 5.1, should be actively pursued.

8. REFERENCES

[1] Hay, Donald A. and Runyon, John P., "Photographs and Resistance
     Measurements of Semi-Submerged Right Parallelepipedons",
     Princeton University, May 1, 1947.

[2] "Research, Investigation and Experimentation in the Field of
     Amphibian Vehicles," Borg-Warner Corporation,
     December 1975.

[3] Hess, John L. and Smith, A.M.O., "Calculation of Non-Lifting
     Potential Flow About Arbitrary Three-Dimensional Bodies,"
     Douglas Aircraft Report No. E.S. 40622, 15 March 1962.

[4] Kotik, J. and Raff, A., "An Application of Wave Drag Theory
     to Ship Design," TRG, Incorporated Report No. TRG-005-FR,
     September 1965.

Security Classification

DOCUMENT CONTROL DATA - R&D
(Security classification of title, body of abstract and indexing annotation must be entered when the overall report is classified)

1. ORIGINATING ACTIVITY *(Corporate author)*	2a. REPORT SECURITY CLASSIFICATION
TRG, A Division of Control Data Corporation	UNCLASSIFIED
	2b. GROUP

3. REPORT TITLE

Amphibious Vehicle Studies

4. DESCRIPTIVE NOTES *(Type of report and inclusive dates)*

Final Report

5. AUTHOR(S) *(Last name, first name, initial)*

Kotik, Jack

6. REPORT DATE	7a. TOTAL NO. OF PAGES	7b. NO. OF REFS
June 1966	41	4

8a. CONTRACT OR GRANT NO.	9a. ORIGINATOR'S REPORT NUMBER(S)
Nonr-4650(00)	TRG-031-FR
b. PROJECT NO.	
c. Task No. NR 062-351	9b. OTHER REPORT NO(S) *(Any other numbers that may be assigned this report)*
d.	

10. AVAILABILITY/LIMITATION NOTICES

Distribution of this document is unlimited.

11. SUPPLEMENTARY NOTES	12 SPONSORING MILITARY ACTIVITY
	Office of Naval Research Department of Navy, Code 438 Washington, D.C.

13. ABSTRACT

This report describes theoretical work aimed at increasing the speed of amphibious vehicles in the water, by decreasing resistance and (if grousers are used for propulsion) improving the flow to the grousers. Alternate mathematical models of the flow were examined and it was concluded that a simple block singularity model gave the best fit to measured resistance data. Although the fit is not very good, and although the mathematical model does not represent the vehicle shape very accurately, it was decided that the model was good enough to serve as a basis for the design of hull modifications intended to reduce drag (and improve the flow to the grouser region). A bulb-like singularity modification was designed mathematically and showed a substantial calculated resistance reduction (Figure 5.1). Due to lack of funds it was not possible to examine the corresponding modified hull shape, nor to conduct any model tests, but the theoretical results suggest that further work in this direction would be profitable.

DD FORM 1473
1 JAN 64

14. KEY WORDS	LINK A		LINK B		LINK C	
	ROLE	WT	ROLE	WT	ROLE	WT
Amphibious vehicles, Wave Resistance reduction.						

INSTRUCTIONS

1. **ORIGINATING ACTIVITY** Enter the name and address of the contractor, subcontractor, grantee, Department of Defense activity or other organization *(corporate author)* issuing the report.

2a. **REPORT SECURITY CLASSIFICATION:** Enter the overall security classification of the report. Indicate whether "Restricted Data" is included. Marking is to be in accordance with appropriate security regulations.

2b. **GROUP:** Automatic downgrading is specified in DoD Directive 5200.10 and Armed Forces Industrial Manual. Enter the group number. Also, when applicable, show that optional markings have been used for Group 3 and Group 4 as authorized.

3. **REPORT TITLE:** Enter the complete report title in all capital letters. Titles in all cases should be unclassified. If a meaningful title cannot be selected without classification, show title classification in all capitals in parenthesis immediately following the title.

4. **DESCRIPTIVE NOTES:** If appropriate, enter the type of report, e.g., interim, progress, summary, annual, or final. Give the inclusive dates when a specific reporting period is covered.

5. **AUTHOR(S):** Enter the name(s) of author(s) as shown on or in the report. Enter last name, first name, middle initial. If military, show rank and branch of service. The name of the principal author is an absolute minimum requirement.

6. **REPORT DATE:** Enter the date of the report as day, month, year; or month, year. If more than one date appears on the report, use date of publication.

7a. **TOTAL NUMBER OF PAGES:** The total page count should follow normal pagination procedures, i.e., enter the number of pages containing information.

7b. **NUMBER OF REFERENCES:** Enter the total number of references cited in the report.

8a. **CONTRACT OR GRANT NUMBER:** If appropriate, enter the applicable number of the contract or grant under which the report was written

8b, 8c, & 8d. **PROJECT NUMBER:** Enter the appropriate military department identification, such as project number, subproject number, system numbers, task number, etc.

9a. **ORIGINATOR'S REPORT NUMBER(S):** Enter the official report number by which the document will be identified and controlled by the originating activity. This number must be unique to this report.

9b. **OTHER REPORT NUMBER(S):** If the report has been assigned any other report numbers *(either by the originator or by the sponsor)*, also enter this number(s).

10. **AVAILABILITY/LIMITATION NOTICES:** Enter any limitations on further dissemination of the report, other than those imposed by security classification, using standard statements such as:

  (1) "Qualified requesters may obtain copies of this report from DDC."

  (2) "Foreign announcement and dissemination of this report by DDC is not authorized."

  (3) "U. S. Government agencies may obtain copies of this report directly from DDC. Other qualified DDC users shall request through
_____ ."

  (4) "U. S. military agencies may obtain copies of this report directly from DDC. Other qualified users shall request through
_____ ."

  (5) "All distribution of this report is controlled. Qualified DDC users shall request through
_____ ."

If the report has been furnished to the Office of Technical Services, Department of Commerce, for sale to the public, indicate this fact and enter the price, if known.

11. **SUPPLEMENTARY NOTES:** Use for additional explanatory notes.

12. **SPONSORING MILITARY ACTIVITY:** Enter the name of the departmental project office or laboratory sponsoring *(paying for)* the research and development. Include address.

13. **ABSTRACT:** Enter an abstract giving a brief and factual summary of the document indicative of the report, even though it may also appear elsewhere in the body of the technical report. If additional space is required, a continuation sheet shall be attached.

It is highly desirable that the abstract of classified reports be unclassified. Each paragraph of the abstract shall end with an indication of the military security classification of the information in the paragraph, represented as *(TS)* *(S)*, *(C)*, or *(U)*

There is no limitation on the length of the abstract. However, the suggested length is from 150 to 225 words.

14. **KEY WORDS:** Key words are technically meaningful terms or short phrases that characterize a report and may be used as index entries for cataloging the report. Key words must be selected so that no security classification is required. Identifiers, such as equipment model designation, trade name, military project code name, geographic location, may be used as key words but will be followed by an indication of technical context The assignment of links, roles, and weights is optional.